Gold/Titania Interfaces and Their Role in Carbon Monoxide Oxidation

Jan-Dierk Grunwaldt and Alfons Baiker*

Laboratory of Technical Chemistry, Swiss Federal Institute of Technology, ETH-Zentrum, CH-8092 Zurich, Switzerland

Received: July 28, 1998; In Final Form: November 9, 1998

The chemisorption properties of differently prepared model gold/titania interfaces have been compared with the aim of gaining a better understanding of the synergistic interplay between the constituents in gold/titania catalysts used in low-temperature CO oxidation. The structurally different gold/titania interfaces were prepared using various techniques, including wet chemical deposition (dip coating) and physical vapor deposition of TiO_2 on flat and highly oriented Au(111)/mica films and immobilization of gold colloids on TiO_2/Au(111)/mica films as well as on TiO_2 powders. The low-temperature activity of small gold colloids anchored on films was corroborated by DRIFTS measurements. CO, CO_2, and O_2 adsorption/desorption studies were performed on the flat model catalysts with TDS, XPS, and ISS. All flat model systems did not show any significant CO adsorption. Oxygen desorption was evidenced by TDS. The adsorptive properties of powder model catalysts were investigated with DRIFTS, pulse thermal analysis, XPS, and ISS. CO adsorption on gold was weak and reversible in all cases and not significantly influenced by the presence of TiO_2. Temperature-programmed desorption of CO_2 indicated that CO_2 was adsorbed if the systems were treated ex situ in oxygen at 673 K. The observed chemisorptive properties of the structurally different gold/titania interfaces support a mechanistic model for CO oxidation which is based on oxygen adsorption on vacancy sites of titania and CO adsorption on gold.

Introduction

Gold is one of the least reactive metals, and has consequently been regarded as relatively unimportant metal in heterogeneous catalysis. However, if gold is finely dispersed on metal oxide surfaces such as TiO_2, ZrO_2, NiO, Fe_2O_3, and Co_3O_4, it exhibits high activity in the low-temperature CO oxidation.[1−4] The activity is strongly dependent on the particle size, the support, and the preparation method.[5−7] In most preparation procedures, the final gold particle size is determined after calcination under oxidizing conditions which lead to more active catalysts than under reducing conditions.

One of the most active catalysts for the low-temperature oxidation of CO is Au/TiO_2. This is particularly interesting because neither bulk Au nor titania is active for CO oxidation at room temperature. Moreover, gold and TiO_2 single crystals have been studied in detail concerning their chemisorptive properties. Both are known to adsorb CO and O_2 weakly. On gold surfaces, only a fractional monolayer of CO is reported to adsorb below 125 K.[8−11] Also adsorption of oxygen occurs only to a small extent on gold surfaces, even at pressures of 2 bar and temperatures between 200 and 500 K.[11−13] Similarly, perfect TiO_2 surfaces are also not covered significantly with CO.[14−17] Some adsorption takes place only in the presence of vacancy defects.[18,19] Also it is supposed that oxygen adsorbs neither on stoichiometric TiO_2 surfaces nor on terraces nor on steps, but on surface oxygen vacancy sites.[14,17,20]

Hence, some synergism between titania and gold seems to be the key for activity. It was proposed that new adsorption sites for CO were created at the interface.[6,7] However, Zhang et al.[21] recently reported on a low-energy ion scattering (LEIS) study of CO chemisorption on Au deposited on a TiO_2 single crystal, concluding that no or only weak CO adsorption was found in this system.

To gain further insight into the role of the gold/titania interface in the low-temperature oxidation of carbon monoxide, we report here on a systematic investigation of the adsorptive properties of structurally different gold/titania interfaces using different model systems, thin flat films, and active powder catalysts.

Experimental Section

2.1. Materials. *Thin-Film Model Systems.* Thin-film model systems were prepared according to the following procedure. First, single crystalline and smooth gold films on air-cleaved muscovite mica were designed in a Bal-Tec BAE 370 vacuum coating system with integrated quartz crystal deposition controller Inficon XTC/2 (Leybold). Further details are given elsewhere.[22] Here the following optimized deposition parameters were used: evaporation rate 0.1 nm/s, film thickness 200 nm, substrate temperature $T_S = 593$ K.

Second, TiO_2 was deposited either by electron beam evaporation or by a wet chemical preparation procedure (dip coating). Electron beam evaporation was performed with a TFI Telemark gun (model 279, 9 kV, ∼30 mA) and TiO_2 (Balzers, tablet, 99.9%) in a graphite crucible. The oxygen partial pressure $p(O_2)$ was varied between 4×10^{-7} and 1×10^{-4} mbar, the substrate temperature T_S between 200 and 620 K. Dip coating was accomplished from titanium tetraisopropoxide solutions in 2-propanol (9 mmol/L − 0.6 mol/L). After immersing an Au(111)/mica sheet (2.0 cm^2 in area) in argon, the samples were hydrolyzed in air. For further details refer to ref.[23] Some of the samples used in this paper are listed in Table 1.

* Corresponding author. Phone: +41-1-632-3153. Fax: +41-1-632-1163. E-mail: baiker@tech.chem.ethz.ch.

10.1021/jp983206j CCC: $18.00
Published on Web 01/23/1999

TABLE 1: Overview of the Samples Used in This Work[a]

sample	layers	characteristics	treatment
ref 1	mica	muscovite mica, freshly split, Baltec	
ref 2	Au(111)/mica	$d = 200$ nm, optimized deposition parameters	
AuTi 1	TiO_{2-x}/Au(111)/mica	TiO_2 on ref 2, $d = 1$ nm, R = 0.01−0.02 nm/s, $T_S = 683$ K, $p(O_2) = 10^{-4}$ mbar	
AuTi 2	TiO_{2-x}/Au(111)/mica	TiO_2 on ref 2, $d = 2$ nm, $r = 0.02$ nm/s, $T_S = 523$ K, $p(O_2) = 4 \times 10^{-6}$ mbar	
AuTi 3	TiO_{2-x}/Au(111)/mica	TiO_2 on ref 2, $d = 10$ nm, $r = 0.05$ nm/s, $T_S = 298$ K, $p(O_2) = 10^{-4}$ mbar	
AuTi 4	TiO_2/Au(111)/mica	TiO_2 on ref 2, $d = 1$ nm, $r = 0.02$ nm/s, $T_S = 298$ K, $p(O_2) = 10^{-5}$ mbar	673 K, in O_2
AuTi 5	TiO_2/Au(111)/mica	TiO_2 on ref 1, dip coating from c(alkoxide) = 9 mmol	
AuTi 6	TiO_2/Au(111)/mica	TiO_2 on ref 1, dip coating from c(alkoxide) = 0.12 mmol	673 K, in O_2
AuTi 7	TiO_2/Au(111)/mica	like AuTi 5, c(alkoxide) = 0.12 mmol	673 K, in O_2
AuTi 8	TiO_2/Au(111)/mica	like AuTi 5, c(alkoxide) = 0.6 mmol	
AuTi 9	TiO_2/Au(111)/mica	like AuTi 5, c(alkoxide) = 0.6 mmol	673 K, in O_2
AuTi 10	Au/TiO_2/Au(111)/mica	Au ($d = 1$ nm) on AuTi 3 (posttreated in oxygen)	
Pow 1	Au_{Col}/TiO_2	gold colloids ($\langle d \rangle = 2$ nm) adsorbed on TiO_2 P25	573 K, in O_2
AuCol 1	Au_{Col}/TiO_2/Au(111)/mica	gold colloids ($\langle d \rangle = 2$ nm) adsorbed on AuTi 3	523 K, in O_2
AuCol 2	Au_{Col}/TiO_2/Au(111)/mica	gold colloids ($\langle d \rangle = 3$ nm) adsorbed on AuTi 7	573 K, in O_2

[a] r = deposition rate, T_S = substrate temperature, $p(O_2)$ = oxygen partial pressure during deposition, d = thickness of the film.

Powder Model Systems. The powder catalysts were prepared via the following steps. First gold colloids were prepared by the reduction of $HAuCl_4$ with THPC (tetrakis(hydroxymethyl)-phosphonium chloride (compare ref 24). Then they were immobilized in acidic medium (pH = 2) on TiO_2 powder (P 25, Degussa). The catalyst was dried for 15 h at 323 K, and further activation was performed by calcination in oxygen at 573 K. Details on this novel preparation procedure, also concerning other supports, will be described elsewhere.[25]

Au_{Col} /TiO_2/Au(111)/Mica. To link both model systems, gold colloids were also adsorbed on TiO_2/Au(111)/mica systems in acidic solution (pH = 2). Both continuous titania (prepared by electron beam evaporation, AuCol 1, Table 1) and highly porous titania films on Au(111)/mica (prepared by dip coating, AuCol 2, Table 1) were used. The composition of the titania films is described in the Results section in connection with the flat model systems. The plates were immersed for about 1 min in the gold sol. Calcination was performed in a similar manner as with the powder model systems.

2.2. Characterization. Structural and chemical properties of the flat model systems were characterized using scanning tunneling microscopy (STM), atomic force microscopy (AFM), scanning electron microscopy (SEM), X-ray photoelectron spectroscopy (XPS), and ion scattering spectroscopy (ISS). Thermal desorption spectroscopy (TDS) in combination with XPS and ISS was applied to investigate their chemisorptive properties. Powder model systems were structurally characterized by means of high-resolution transmission electron microscopy (HRTEM) and XPS. Diffuse reflection infrared Fourier transform spectroscopy (DRIFTS), pulse thermal analysis (PTA), XPS, and ISS were used to study their chemisorptive properties.

AFM and STM images were taken with a Topometrix TMX 2000 system as described in ref 22. Scanning electron micrographs of the thin films were obtained using a JEOL JSM 840 microscope. The samples were imaged with a 15 keV beam, in most cases with an angle of 20°, without any treatment of the sample due to the high electrical conductivity of the substrate.

HRTEM images of the gold particles were obtained using a JEOL 2010 electron microscope with a LaB_6-cathode operated at an accelerating voltage of 200 kV. Powder particles were suspended in ethanol for about 1 min under ultrasonic treatment and were then dropped onto a carbon film copper grid. In the case of thin films, the oxide support with gold colloids on top of it was directly transferred to the grid of the microscope.

For surface analysis with XPS and ISS as well as for the study of chemisorptive properties with TDS, a multipurpose, multichamber UHV apparatus with load lock, preparation, high pressure, and analysis chambers was set up. The different chambers were connected via a transfer chamber with radial transfer system, suitable for thin films as well as for powder samples. Powder samples were mounted on a temperature-controlled sample holder (Leybold) with resistive heating (120 to 873 K), the temperature being measured below the sample. For thin film models, a home-built sample holder was used and the samples (5×5 mm^2 − 10×10 mm^2) were attached to a thin molybdenum foil. The sample was heated by a combination of irradiation and electron impact from a tungsten filament, located at the rear side of the sample and tuned by a Eurotherm controller for linear heating rates (0.5−7.5 K/s, up to 1273 K). The temperature was measured by a thermocouple spot-welded on the thin molybdenum foil directly beneath the sample. Both sample holders could be cooled to 120 K by connecting them to a liquid nitrogen reservoir. The samples were introduced into the chamber via a load lock (slow evacuation and aeration for powder samples) and normally outgassed for about 12 h at room temperature.

Spectroscopic analysis was performed on a Leybold Heraeus LHS 11 MCD instrument (analysis chamber) containing an X-ray source RQ 20/38 (Specs) for XPS-analysis, a two-step differentially pumped ion gun (IQE 12/38, Leybold) used for ion scattering spectroscopy (He^+, 1 keV), a hemispherical analyzer EA 11 MCD (Leybold), a quadrupole mass spectrometer used for residual gas analysis, and a flood gun. Thermal desorption spectroscopy was performed in the preparation chamber using a quadrupole mass spectrometer (Leybold PGA 100) with Feulner Cup. The detection limit was estimated to be lower than 0.01 monolayers, if one assumes a flat film of 25 mm^2. The TDS setup was tested with tungsten samples, as well as Pt/mica and Ag/mica samples. Sputtering could be performed either with the ion gun for ISS in the analysis chamber or with a Penning source IQP 10/63 (Leybold) in the preparation chamber. The high-pressure chamber was used for degassing powder samples at elevated temperatures and for dosing different gases at high partial pressures. Adsorption experiments, analyzed with XPS or ISS, were directly performed in the analysis chamber at 120 K. ISS is more surface sensitive than XPS. An upper detection limit strongly depends on the substrate. In case of a completely flat oxide with Au on top of it, ISS would be more sensitive than 0.05 ML as described by Zang et al.[21]

Diffuse reflectance FTIR spectra were recorded on a FTIR instrument (Perkin−Elmer, model 2000) containing a diffuse reflection unit and a reaction cell (both Spectra-Tech) equipped with ZnSe windows (permeable > 700 cm^{-1}). The powder

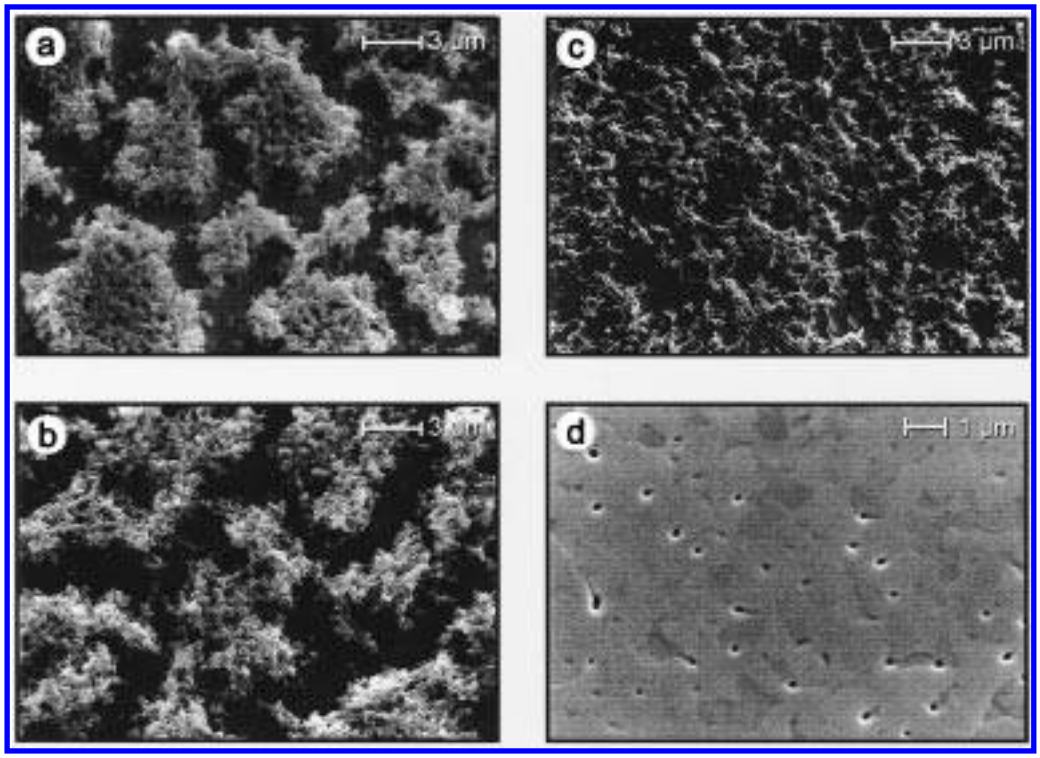

Figure 1. Scanning electron micrographs of TiO_2 on Au(111)/mica prepared by dip coating from titanium tetraisopropoxide solutions: (a) 0.6 mol/L; (b) 0.4 mol/L; (c) 0.05 mol/L; (d) 0.009 mol/L.

sample was mounted on an Al_2O_3 frit which could be heated to elevated temperatures (here 573 K) via a PID controller (Tecon 580). In the case of thin films, a small hexagonally cut plate (d $\sim$ 5 mm) was adhered to the top of the frit. Further details on the apparatus can be found in ref 26. The samples were held for more than 2 h in an Ar stream (50 mL/min) prior to measurement to remove traces of water. In situ calcination was performed in oxygen (40% O_2 in Ar, 99.999%, Pangas) with a heating rate of 5 K/min and a dwell time of 30 min. Adsorption studies were carried out using a gas flow of 6 mL/min (5200 ppm CO in He). All gases were dried with a cooling trap containing dry ice/2-propanol.

Steady-state catalytic tests were conducted in a glass microreactor using a reaction mixture of 2500 ppm CO (99.997%, Pangas) and 2500 ppm O_2 (99.999%, Pangas) in a nitrogen balance (CO feed rate of to 2.5×10^{-7} mol s^{-1} g_{cat}^{-1}).

Thermoanalytical investigations (DSC/TG) were carried out using a Netzsch STA 409 thermoanalyzer equipped with a gas injector for pulse thermal analysis (PTA)[27] enabling injection of small amounts of pure gases or gaseous mixtures (0.25 to 1.0 mL) into the system. Evolving gases were monitored online with a Balzers QMG 420 quadrupole mass spectrometer which was connected to the thermoanalyzer by a heated (ca. 573 K) capillary.

Results

3.1. Thin-Film Model Systems. *3.1.1. Structural Characterization.* The topography of the gold films, prepared after optimization of the deposition parameters, was smooth with atomically flat terraces and single crystalline, predominantly exhibiting (111) planes. Some results have recently been reported in ref 22 and are similar to those of other authors.[28,29] These films are highly conductive, useful for spectroscopic investigations, and contain only small amounts of oxygen (<2%). They are suitable for producing the metal oxide/gold interface by different techniques including wet chemical methods.

TABLE 2: XPS Data of Dip-Coated and Evaporated TiO_2/Au(111)/Mica Samples

sample	treatment in UHV	C 1s [at%]	O 1s [at%]	Ti 2p [at%]	Au 4f [at%]
AuTi 1	673 K	20.9	50.6	17.4	11.1
AuTi 2		14.0	54.0	22.6	9.3
AuTi 4		13.4	39.1	16.0	31.5
AuTi 4	673 K	11.7	37.5	17.5	33.4
AuTi 4	673 K, sputtering for 12 min with He^+	11.9	33.4	16.0	38.7
AuTi 5		33.3	50.9	12.6	3.2
AuTi 5	673 K	24.9	53.4	16.6	5.1
AuTi 6		16.6	59.0	17.5	7.0
AuTi 6	673 K	11.3	62.0	18.2	8.5
AuTi 8		19.2	57.9	18.6	4.3
AuTi 9		16.7	51.5	14.9	17.0

The deposition of TiO_2 onto these Au(111)/mica substrates by dip coating resulted in films with different morphology depending on the precursor concentration in the solution and on the posttreatment. In Figure 1, typical scanning electron micrographs of samples coated with solutions of different concentration are shown, revealing that at higher concentrations (>0.01 mol/L) small, highly porous islands are formed during evaporation of the liquid affording a discontinuous film. At lower concentrations (<0.01 mol/L) a thin continuous film is obtained. AFM studies corroborated the SEM findings. The presence of Ti on the surface was confirmed by XPS (Table 2) and ISS. The sputter profile of the thin continuous film is depicted in Figure 2a and compared to different electron beam evaporated films (Figure 2b,c).

Formation of two kinds of particles during deposition can be explained by two mechanisms.[30] In both cases, a thin liquid film forms upon dip coating. Evaporation of the liquid leads to the formation of droplets where the concentration reaches a certain level of supersaturation in the case of highly concentrated solutions and nuclei are spontaneously formed. From these nuclei crystals start to grow in the droplets. As the concentration

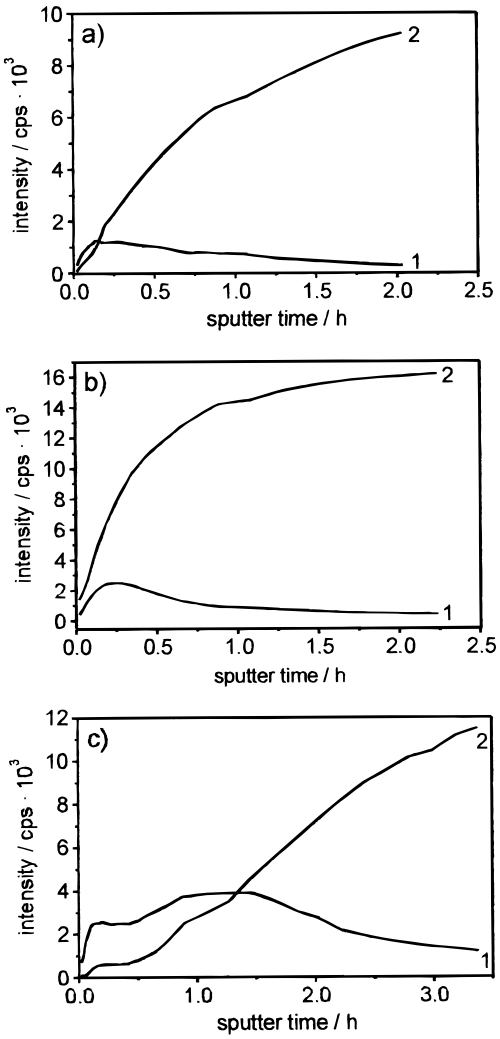

Figure 2. ISS sputter profiles of TiO_2 films (1: titanium, 2: gold) prepared by (a) dip coating, $c = 0.009$ mol/L, posttreatment at 393 K, 1 bar oxygen (AuTi 5); (b) electron beam evaporation, $d = 2.0$ nm, $T_S = 298$ K; (c) electron beam evaporation, $d = 10.0$ nm, $T_S = 298$ K.

of the solution decreases, formation of further nuclei is prevented. In the case of diluted solutions the dissolved alkoxide does not nucleate in separate particles but forms a homogeneous film.

The morphology of the highly porous films changes during calcination, as followed by AFM and SEM, due to sintering effects, accompanied by crystallization to anatase around 850 K. The crystallization was confirmed by XRD and Raman spectroscopy (characteristic bands at 400 cm^{-1}, 515 cm^{-1} and 637 cm^{-1}). Sintering is also reflected in the XPS data in Table 2 (AuTi 8, uncalcined, and AuTi 9, calcined at 673 K, see Table 1). The film thickness of the continuous film was estimated to be about 2 nm, by comparing the sputter profiles (Figure 2a) to those of the electron beam evaporated films (Figure 2b,c), the thickness of which has been controlled during deposition.

The deposition of TiO_2 by electron beam evaporation, dependent on the oxygen partial pressure in the system, has been reported in a previous study.[23] It was concluded that fully oxidized TiO_2 films can be prepared at $p(O_2) > 4 \times 10^{-5}$ mbar. XPS data of different TiO_2 films on Au(111)/mica are listed in Table 2. The substantial amount of gold on the surfaces of 1 and 2 nm thick films (AuTi 1, AuTi 2) shows that both gold and titania are present on the surface and that TiO_2 grows via an island mechanism on the gold surface. The low spreading of metal oxides on gold has been reported previously and is due to the high interfacial energy between the two phases.[31,32] Also with ion scattering spectroscopy, which is much more surface sensitive than XPS, a significant amount of gold was detected. Hence, TiO_2 tends to cluster into 3D particles resulting in a pronounced gold/metal oxide interface, which is a suitable model to start with. In the case of a 10 nm thick TiO_2 film, no gold is detected by ISS (Figure 2c), indicating that TiO_2 covers the whole gold substrate. Further use of this substrate by deposition of gold colloids on these flat metal oxide films is described in Section 3.3. In all cases, the deposited TiO_2 did not show any charging effects in XPS due to the conductivity of the gold substrate, which makes them additionally interesting models for the gold/oxide interface.

3.1.2. Adsorption of CO and O_2 on Mica and Au(111)/Mica. After adsorption of CO, CO_2, and O_2 on freshly split muscovite mica and Au(111)/mica, TDS did not show any desorption peaks between 150 and 600 K. The linear heating rates were varied between 0.5 and 5 K/s. At higher temperatures, the mica started to lose some oxygen (>900 K). Discrimination between the CO signal and the background signal was improved by using ^{13}CO. The absence of significant CO adsorption is in accordance with the literature, where it is stated that CO only weakly adsorbs on Au at temperatures lower than 125 K.[8−11] Also on muscovite mica, no adsorption is known in this temperature range and therefore it was used for a variety of former TDS studies.[33−36]

3.1.3. Adsorption of CO, CO_2, and O_2 on TiO_2/Au(111)/Mica. For adsorption experiments, studied with TDS in combination with XPS and ISS, mainly the thin metal oxide films prepared by dip coating (AuTi 5) and electron beam evaporation (AuTi 1) were used. Some of the samples were posttreated in air (Table 1). The entire study included thinner and thicker metal oxide deposits as well as differently ex situ and in situ treated films.

Both the electron beam evaporated and dip-coated films (AuTi 1, AuTi 2, AuTi 5) did not show adsorption of CO, CO_2, and O_2 (0.5−50 L CO or O_2) at 120 K in the temperature range 150−600 K (heating rates 1.0−7.5 K/s) within the detection limit of the methods used. Also no significant coadsorption of CO and O_2 occurred. The data from XPS analysis of some samples during different stages of the experiments are shown in Table 2 and indicate that the carbon content decreased mainly after the first heating cycle. Hence, some samples were outgassed at 673 K prior to adsorption experiments.

Moreover, it was mentioned in the Introduction that the preparation of the real catalysts requires an oxidative treatment for activation. Therefore, some samples were posttreated ex situ in oxygen at 673 K and then used for investigations (AuTi 4 and AuTi 6). The gold content, as determined by XPS (Table 2) and ISS, significantly increases in both cases (AuTi 4 compared to AuTi 1 and AuTi 6 compared to AuTi 5), illustrating that the adhesion energy is low in the gold/oxide system. Note that in UHV, the samples were only heated to 673 K for short times, whereas ex situ the samples were held at 673 K for 1 h which allows greater restructuring of the sample. Additionally, the XPS signal of the hydroxyl groups, located on the higher binding energy site of the O1s peak, decreased significantly during posttreatment.

Also on these differently treated interfaces no CO desorption was found after CO adsorption at 120 K using heating rates between 1.0 and 7.5 K/s. Only at the beginning of the desorption experiment did some CO desorb, probably an artifact of adsorption on the sample holder. However, we found significant adsorption of CO_2 on these samples as shown in Figure 3 and 4. Even CO_2 arising from the background during CO adsorption

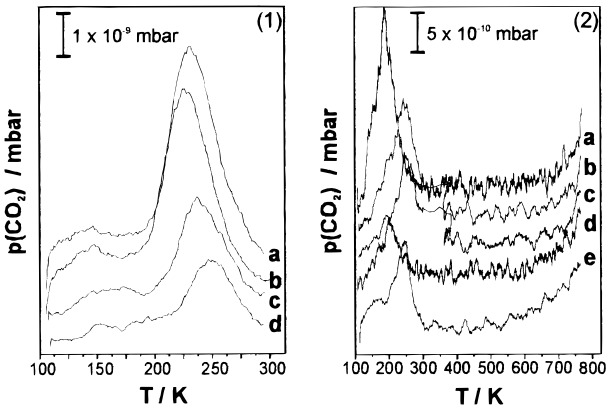

Figure 3. Desorption of CO_2 from the TiO_2/Au(111)/mica model sample AuTi 3 (1) and from the same, but sputtered sample (2) after adsorption of CO at 110 K. Sample (1), heating rates 5 K/s; adsorption of (a) 13.0 L, (b) 10.0 L, (c) 4.5 L, (d) 3.5 L; sample (2) with the following conditions: (a) 3.5 L, 5 K/s (directly after sputtering); (b) 14.0 L, 5 K/s; (c) 2.0 L, 5 K/s; (d) 2.0 L, 2 K/s; (e) 14.0 L, 2 K/s.

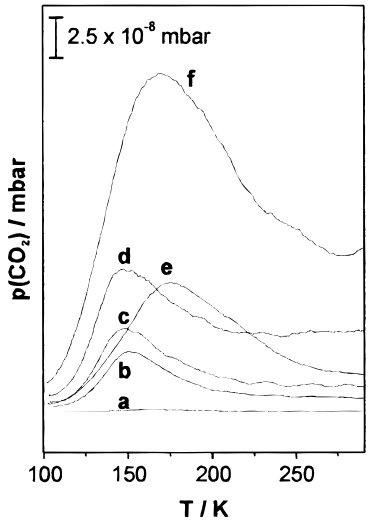

Figure 4. Desorption of CO_2 after adsorption of CO_2 on an electron beam evaporated TiO_2 film on Au(111)/mica (AuTi 3): (a) 0 L, 2 K/s (between different adsorption steps); (b) 1.6 L, 2 K/s; (c) 2.5 L, 2 K/s; (d) 8.5 L, 2 K/s; (e) 2.5 L, 5 K/s; (f) 7.5 L, 5 K/s.

was adsorbed on the sample (Figure 3). By using ^{13}CO we could rule out that $^{13}CO_2$ formation took place during CO adsorption at 120 K, even if oxygen was coadsorbed.

Sputtering of the samples with He^+ during ion scattering spectroscopy (Figure 5) or heating of the sample to 973 K in UHV (not shown) resulted both in much lower CO_2 adsorption. The ISS sputter profiles are shown in Figure 5, indicating that the gold content significantly increased during sputtering. Nevertheless, no increase of CO adsorption was found.

The appearance of CO_2 in the desorption spectrum is probably associated with the formation of some surface carbonate on TiO_2 which has been reported to decompose at rather low temperatures in UHV.[37] Moreover, it is known that CO_2 adsorbs to some extent on TiO_2 surfaces.[14,17] In the case of AuTi 1, hydroxyl groups are present on the surface as evidenced by XPS (not shown) which could result in a more stable carbonate. The formation of a bicarbonate species as a consequence of the presence of surface hydroxyl groups has been reported by Tanaka and White.[19]

Both procedures, heating to 973 K and sputtering with ISS, resulted in reduction of surface Ti^{4+} as shown by XPS (Figure 5). The reduction of surface Ti^{4+} to Ti^{3+} can be another reason

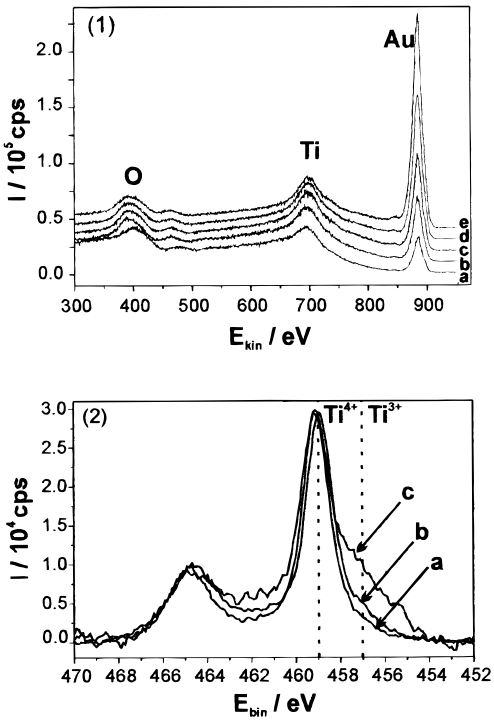

Figure 5. (1) Successive ISS spectra of TiO_2/Au(111)/mica model sample AuTi 3 which were recorded between two TDS experiments. (2) Ti 2p XP spectra: a, before sputtering; b, after heating to 973 K; c, after 5 sputter cycles (time 11:45 min).

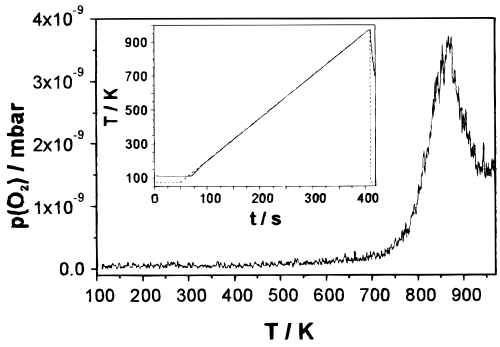

Figure 6. Desorption of O_2 from sample AuTi 3 (heated to 773 K before in UHV and during TDS), temperature ramp shown as inset.

for the lack of desorption of CO_2 after both treatments in TDS. Interestingly, desorption of oxygen starts at ca. 800 K in the O_2 TDS spectrum (Figure 6) which is significantly lower than the temperature for oxygen loss from TiO_2. During further cycles no additional oxygen desorbs, even after long O_2 adsorption (40 L, 120 K).

To underline the observation that CO is not adsorbed on the gold/oxide model systems, CO adsorption was also studied using XPS and ISS at 120 K. In both cases no decrease of the gold peak after adsorption of CO (20 L) at 120 K was observed. Diffuse reflectance FTIR experiments were not found to be useful at room temperature with a partial pressure of CO around 5 mbar (in argon), because the doublet of gaseous CO centered at 2150 cm^{-1} was much stronger and overlapped with the typical bands of linearly bonded CO on gold around 2115 cm^{-1}. After flushing with argon no detectable CO adsorption band remained in the spectrum.

3.2. Powder Model Systems. *3.2.1. Structural Characterization.* Figure 7 shows the structure and size of the gold particles in solution when prepared by reduction with THPC and after their immobilization on TiO_2. The size was around 2 nm and

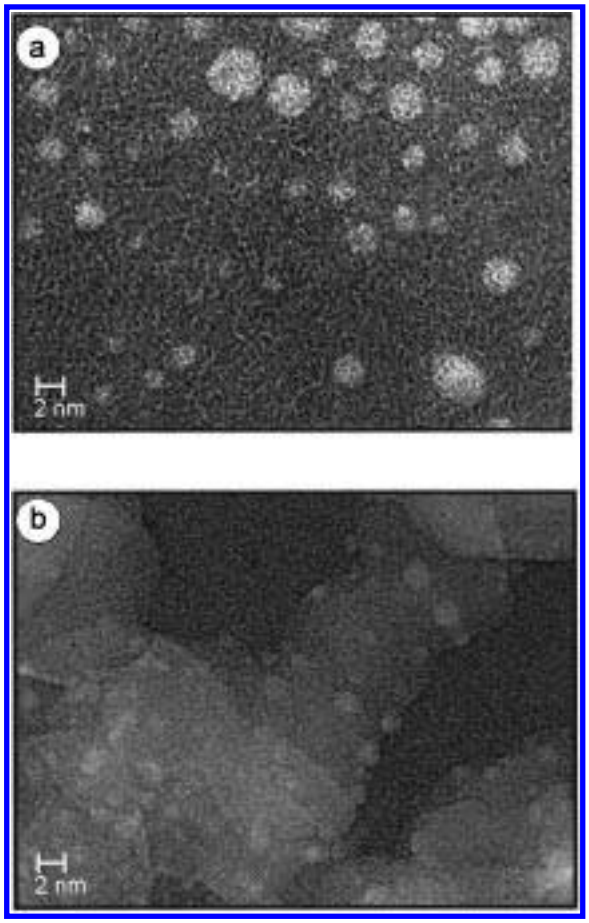

Figure 7. HRTEM images: (a) gold colloids in solution before adsorption on the metal oxide support; (b) Au/TiO_2 (1.7 wt % Au, Pow 1).

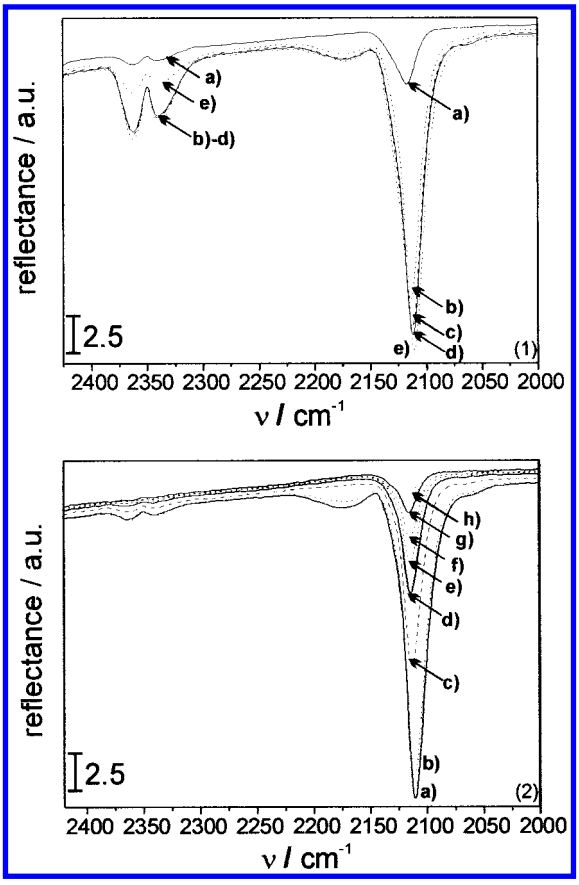

Figure 8. DRIFT spectra of CO adsorption and desorption on Au/TiO_2 (1.7 wt % Au, Pow 1, heated ex situ to 573 K in 1 bar O_2): (1) Adsorption of CO after (a) 2 min, (b) 4 min, (c) 6 min, (d) 8 min, (e) 20 min. (2) Desorption of CO after (a) 0 min, (b) 2 min, (c) 4 min, (d) 6 min, (e) 8 min, (f) 10 min, (g) 14 min, (h) 18 min.

was nearly preserved during deposition. Also in the case of higher loadings, only partial aggregation of the gold particles occurred.

The investigation of the catalytic activity of the Au/TiO_2 catalyst (1.7 wt % Au, Pow 1) uncovered that the uncalcined catalyst was active without further activation (Table 3). After heating the reaction mixture to 423 K, the catalyst was much more active. Calcination at 573 K resulted in an even more active catalyst (Table 3). In 20% oxygen, 100% conversion was obtained after both treatments at room temperature. Haruta[6] reported that moisture enhances activity. However, we found on the investigated catalysts a strong decrease in activity when only small amounts of water were introduced and consequently enhanced activity could be due to removal of water in the as-prepared catalyst. This behavior is supported by recent results from Bollinger and Vannice[7] who also observed a decrease in activity on Au/TiO_2 catalysts (prepared by deposition−precipitation) if water was introduced. Another reason could be a stronger contact between Au particles and TiO_2 due to the heat treatment, as claimed by Haruta.[6] Finally, it is interesting to note that gold particles supported on titania exhibited higher activity than those supported on zirconia even if the particle size and loading were the same, as will be discussed in detail in ref 25.

3.2.2. Adsorption Experiments on Powder Au/TiO_2. The adsorption of CO on the powder model systems has been studied with DRIFT spectroscopy and pulse thermal analysis at elevated CO partial pressures and compared to XPS and ISS results of the adsorption behavior of CO on gold and/or the interface at low temperatures under UHV conditions.

Figure 8 shows the typical DRIFT spectrum of a catalyst (Pow 1, 1.7 wt % Au), treated at 573 K ex situ and exposed to air before introduction into the IR cell. The corresponding spectrum of the same catalyst, but heated in situ in oxygen, is depicted in Figure 9. Both spectra reveal that CO binds reversibly on the surface at room temperature. The bands for adsorbed CO around 2115 cm^{-1} are indicative for linearly adsorbed CO on gold.[7,38−41] Moreover, a shoulder at higher wavenumbers is observed, which could be due to adsorption of CO on positively polarized gold sites.[38,42,43] This shoulder is much more pronounced in the case of the in situ treated catalyst and some additional features are found (Figure 9). The band located at 2180 cm^{-1} is attributed to the adsorption of CO on Ti^{4+} sites.[44,45] The band around 2350 cm^{-1} is associated with adsorbed CO_2, as already reported on oxidized gold electrodes.[38,46,47] Its intensity slowly decreases with longer exposure, and the catalyst is not fully active directly after prolonged oxygen treatment.

TABLE 3: Activity of Au/TiO_2 (1.7 wt % Au) at Different Stages of Posttreatment

sample description	temperature	conversion
uncalcined sample (dried for 15 h at 323 K)	303 K	21%
uncalcined sample	353 K	100%
uncalcined sample after heating till 423 K in the reaction mixture	304 K	68%
calcined sample (573 K)	298 K	90%

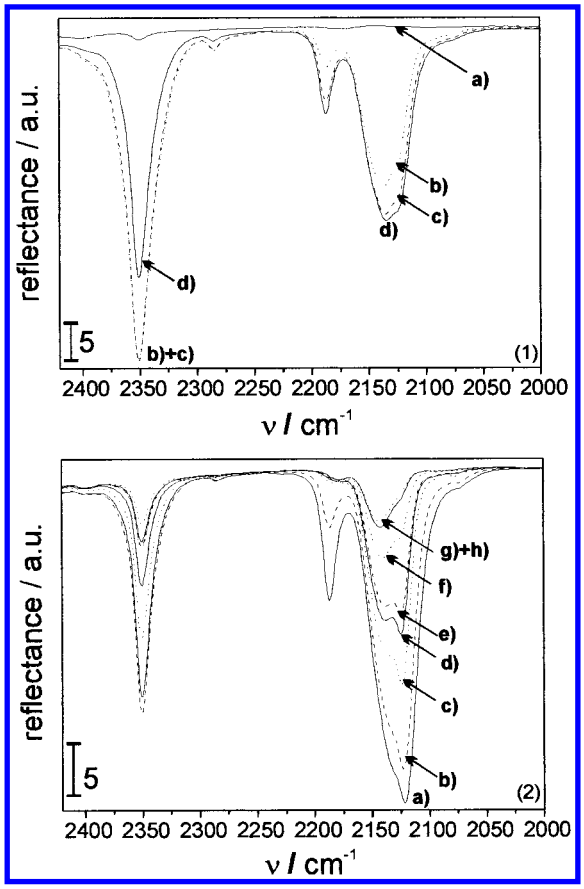

Figure 9. DRIFT spectra of CO adsorption and desorption on Au/TiO_2 (Pow 1, heated in situ to 573 K in 40 % O_2 in Ar): (1) Adsorption of CO after (a) 2 min, (b) 4 min, (c) 6 min, (d) 16 min. (2) Desorption of CO (later cycle) after (a) 0 min, (b) 2 min, (c) 4 min, (d) 6 min, (e) 8 min, (f) 10 min, (g) 12 min, (h) 16 min.

Note also the formation of free CO_2 in the beginning of the CO exposure shown in Figure 8.

The typical behavior of two samples in pulse thermal analysis is shown in Figures 10 and 11. Here, higher loaded catalysts (16.6 wt % Au) were used, so that changes in mass due to adsorption are more easily detected. Figure 10 shows that no detectable weight changes were observable in the TG curve around 359 K if CO, O_2 or CO_2 pulses are used. The apparent weight loss during the pulse is due to the buoyancy effect caused by the change in gas density. Note that during a CO pulse also some CO_2 is formed, indicating that the crude catalyst is active at low temperature. After catalyst activation at 743 K in oxygen, the behavior of the catalyst changed when exposed to a CO pulse (Figure 11). More CO_2 was formed and some weight gain was indicated by the TG curve. However, quick desorption occurred over a time scale of a few minutes.

Under UHV conditions, adsorption of CO was performed in the following way. The sample was cooled to about 120 K and then CO was dosed (about 20 L). Under these conditions, no adsorption of CO was indicated by ISS and XPS. If CO adsorption occurred on gold atoms at the interface a reduction of the gold signal (in XPS Au 4f peak) is expected connected with the increase of a carbon signal (in XPS C 1s signal around 286 eV and a shake-up satellite at 292 eV, e.g., refs 48 and 49). The sensitivity should be sufficient in the case of gold (the C 1s signal is disturbed by carbonaceous impurities) and even adsorption on gold atoms at the interface might be detectable in the case of CO adsorption because the number of gold atoms located at the interface is high. However, no significant decrease of the gold signal was found. Also with ISS, no adsorption was

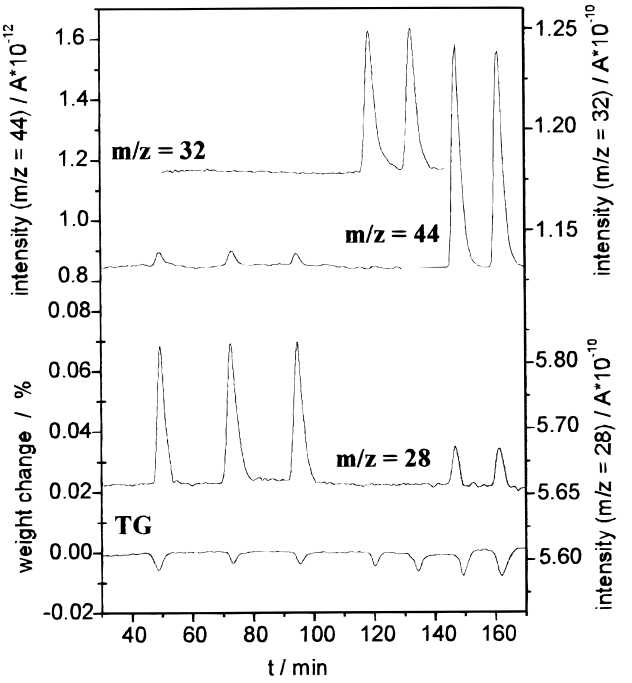

Figure 10. Pulses of CO ($m/z = 28$), O_2 ($m/z = 32$), and CO_2 ($m/z = 44$) over Au/TiO_2 (16.6 wt %) at $T = 359$ K—activated during heating under oxygen to 400 K. The last two pulses of CO_2 were used for quantitative calibration of the mass spectrometric signal of $m/z = 44$, note the change of the intensity scale.

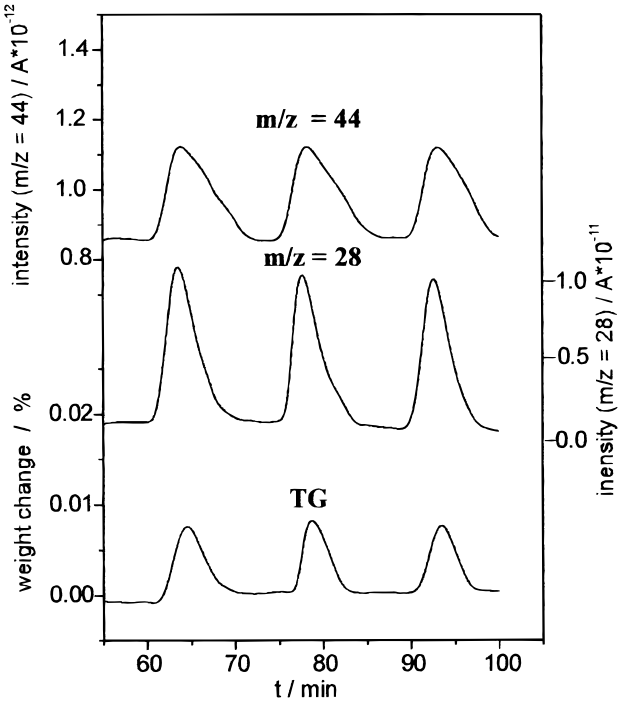

Figure 11. Change of mass (TG) and formation of CO_2 ($m/z = 44$) resulting from CO pulses ($m/z = 28$) at 330 K over Au/TiO_2 (16.6 wt %) after in situ activation by heating under oxygen to 743 K (10 K/min).

detected. The intensity of gold in this case was low, and charging effects occurred.

3.3. Flat Au_{Col}/TiO_2/Au(111)/Mica Model Systems. *3.3.1. Structural Characterization.* The immobilization of gold colloids on TiO_2 films was performed analogously to that on the powdered model systems. Instead of using TiO_2 powder, the continuous TiO_2 film on Au(111)/mica (AuTi 3) or the highly

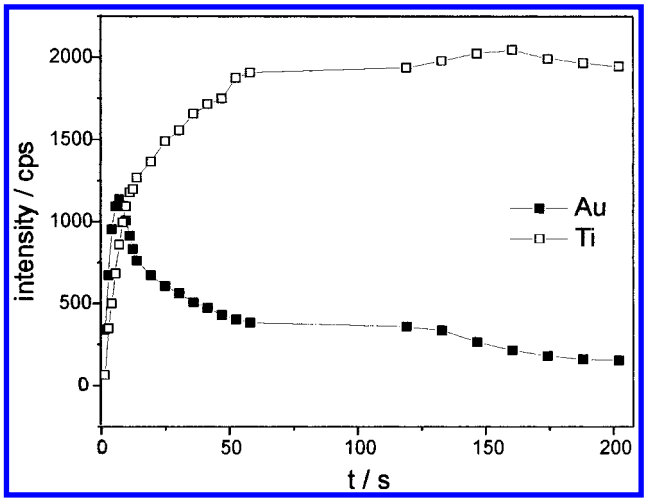

Figure 12. Sputter profile of sample AuCol 1 with Ti (closed square) and Au (open square).

porous TiO_2 film on Au(111)/mica (AuTi 7) was used as substrates. The adsorption of gold colloids in acidic solutions proceeded on all substrates, as evidenced by XPS (1−2 at. % Au) and ISS in the case of the continuous TiO_2 film (Figure 12) and additionally by a HRTEM image of the more porous TiO_2 film (Figure 13c). In the first case (AuTi 3), gold particles of about 2 nm (as depicted in Figure 7a) were immobilized. The corresponding ISS spectrum in Figure 12 demonstrates that the gold colloids were mainly located on the surface because scattering on gold atoms occurred mainly in the beginning of the sputter profile. In the second case (AuTi 7), larger gold particles in the range of 3−4 nm were used (Figure 13a) and deposited on the porous film, whose SEM image is depicted in Figure 13b. Since the TiO_2 layer was rather thick, the gold colloids with the TiO_2 deposits could be directly transferred onto the carbon coated grid. Figure 13c indicates that the size of the supported gold particles was also preserved during this process. The contrast of the TiO_2 support in the HRTEM image (Figure 13c) is less pronounced compared to the powder catalyst (Figure 7b) because it was less crystalline. Imaging of the gold colloids on the oxide and on the underlying Au(111) substrate also showed that the gold colloids were mainly located on the surface of the oxide and not in its pores or on the Au(111) support. This is supported by ISS sputter profiles showing only a strong Au signal in the beginning (not depicted). Since the models are electrically conducting and flat, they are interesting model systems for further investigation of the gold/oxide interface.

3.3.2. Adsorption Experiments on $Au_{Col}/TiO_2/Au(111)/Mica$. The flat $Au_{Col}/TiO_2/Au(111)$/mica system (AuCol 1) did not show any other desorption behavior in TDS compared to the results reported above for the $TiO_2/Au(111)$ model system. Data from XPS analysis are depicted in Table 4. Interestingly, also in ISS and XPS before and after adsorption of CO at 120 K, no significant change of the signals was observed. In particular, the gold signal was expected to decrease significantly in both cases if CO adsorption occurs.

Since the surface area of this first model catalyst (AuCol 1) was low and the band of gaseous CO in diffuse reflectance FTIR spectroscopy was too strong, no signal could be detected in DRIFTS. Hence, the question arises, as to whether such flat model systems are catalytically active systems which mimic gold catalysts. For this purpose, the highly porous film of TiO_2 on gold, prepared by dip coating, was investigated in further detail.

The investigation of CO adsorption on AuCol 2 at room temperature with DRIFTS is depicted in Figure 14. It shows again that the typical bands for adsorbed CO are much smaller than the doublet of free CO centered around 2150 cm^{-1} (Figure 14.1a), as in the case of the other model catalysts. Moreover, desorption in Ar was too rapid compared to the real catalysts (Figure 14.1b−d). However, it could be proved indirectly that they are suitable model systems. When exposed to a mixture of CO (ca. 3000 ppm) in O_2 (ca. 15%) they exhibited a

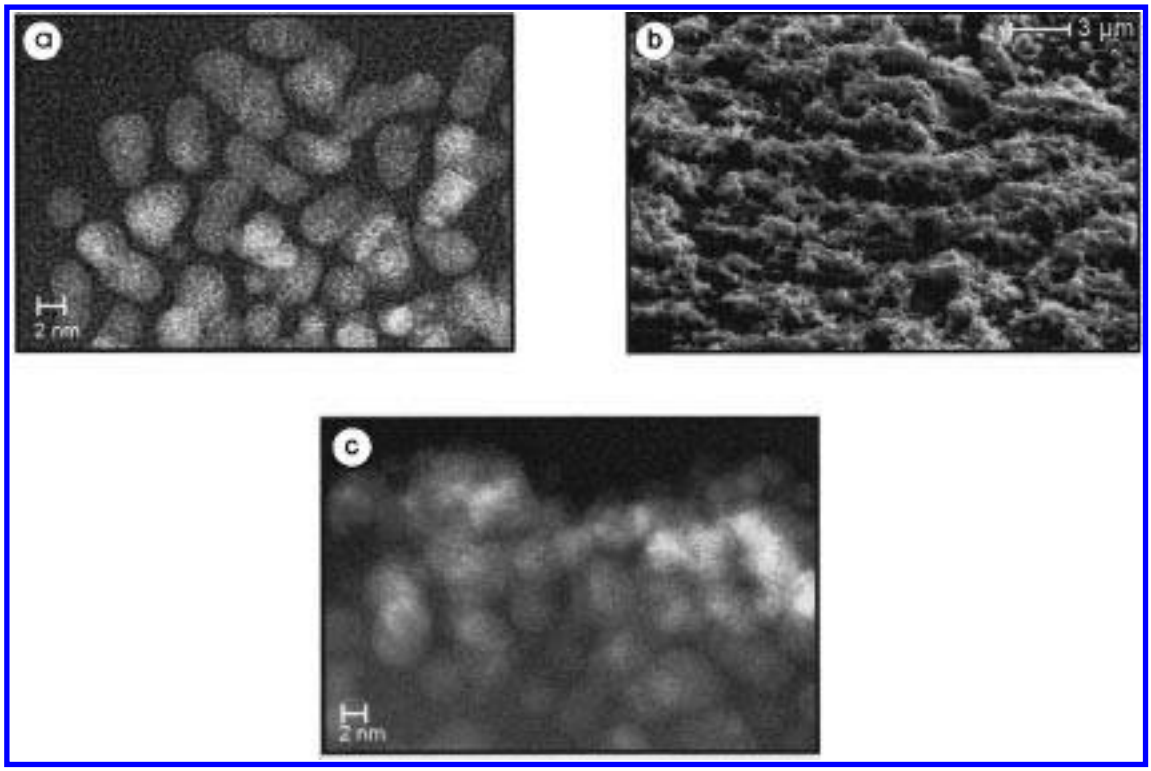

Figure 13. (a) HRTEM image of the gold colloids used for immobilization; (b) SEM image of the dip-coated TiO_2 film, AuTi 6 (c(alkoxide)) = 0.12 mol/L, posttreated in oxygen at 393 K; (c) HRTEM image of gold colloids on a dip-coated TiO_2 film on Au(111)/mica (AuCol 2).

TABLE 4: XPS Data of $Au_{Col}/TiO_2/Au(111)/Mica$ Samples

sample	treatment in UHV	C 1s [at%]	O 1s [at%]	Ti 2p [at%]	Au 4f [at%]
AuCol 1		20.3	62.7	15.8	1.2
AuCol 1	673 K	13.9	63.0	21.6	1.5
AuCol 1	at 120 K, after CO adsorption, 22 L	14.3	62.9	21.3	1.5
AuCol 2		33.1	56.6	8.2	2.1
AuCol 2	after sputtering with ISS (6 min)	25.1	60.4	11.5	3.0

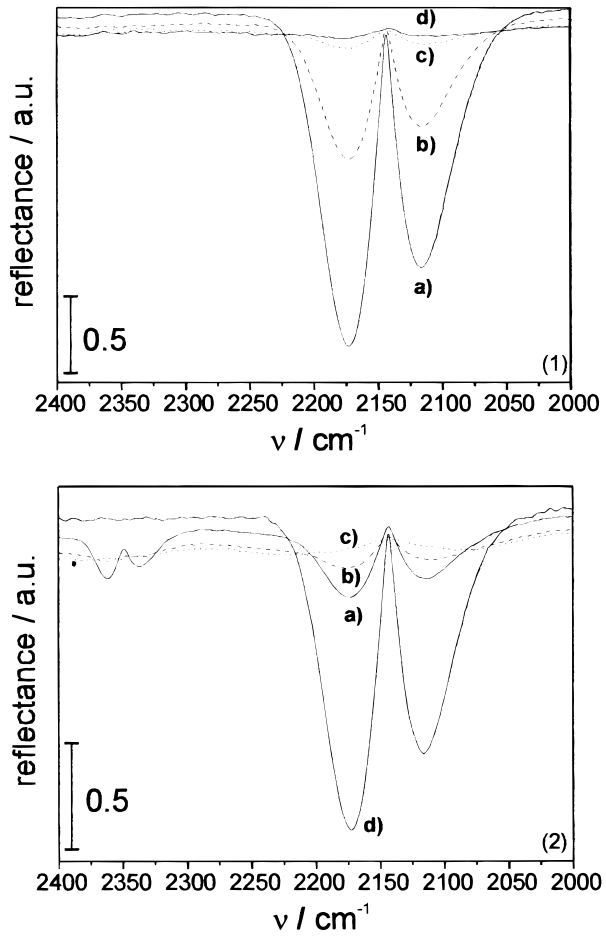

Figure 14. DRIFT spectra of (1) CO desorption from $Au_{Col}/TiO_2/Au(111)/mica$ (AuCol 2, calcined ex situ at 523 K in O_2, exposed to 5200 ppm CO in Ar): after (a) 0 min, (b) 2 min, (c) 4 min, (d) 6 min; (2) $Au_{Col}/TiO_2/Au(111)/mica$ (AuCol 2, calcined ex situ at 523 K in O_2) under reaction conditions (ca. 3000 ppm CO and 15% O_2 in Ar, steady state) − switch to O_2 (40 % O_2 in Ar): after (a) 0 min, (b) 2 min, (c) 4 min, (d) Au(111)/mica sample (ref 2, Table 1) under reaction conditions (the same conditions as in 2a).

significant band of free CO_2 (Figure 14.2a). This band was much smaller if 2500 ppm O_2 and 2500 ppm CO were passed over the film. Since such a band, indicative of free CO_2 was not found with CO or O_2 alone (e.g., due to impurities) and with a Au(111)/mica reference sample (Figure 14.2d), this indicates that CO_2 is formed at room temperature on such a model film. If the film (AuCol2) was treated in oxygen before use in the DRIFTS cell, traces of CO_2 formed upon CO exposition although the model film catalyst was held in an Ar gas stream in the IR cell before use for more than 2 h. This behavior has also been observed for the calcined Au/TiO_2 powder catalyst.

The investigation of the flat model system (AuCol2) under UHV conditions resulted in the following observations. Using TDS, no pronounced desorption band was detected (adsorption of 1−20 L of CO) although there was a broad feature around 220 K which could be due to some adsorption of CO. Also coadsorption of O_2 and CO at such low temperatures did not result in CO or CO_2 desorption and with ISS and XPS no decrease of the gold signal was detected after CO adsorption.

Discussion

We have compared the chemisorptive properties of differently prepared gold/titania interfaces with the aim to gain new insight into the synergistic interplay between gold and TiO_2 utilized in low-temperature CO oxidation. Whereas the presented powder model systems exhibit high activity in the low-temperature CO oxidation, comparable to results obtained on catalysts prepared via deposition−precipitation and coprecipitation,[2,7] the flat TiO_2/Au(111) model systems provide gold/titania interfaces, which are conductive and suitable for TDS experiments. The preparation procedure via gold colloids not only offers the advantage to control the final gold particle size before deposition, but also is transferable to a flat model system, as evidenced by immobilizing gold particles of definite size on a flat metal oxide support. DRIFT spectroscopic measurements confirmed the activity of these planar model catalysts in the CO oxidation. This may add another example to the few examples known[36,50−52] where the "structure gap" between surface science model systems and powder model catalysts could be nearly bridged. Valden et al. have very recently prepared a single crystalline $Au/TiO_2(110)$ model system which complements the existing models for the $Au-TiO_2$ interface from the surface science side.[58]

Both single crystalline gold surfaces and TiO_2 are known to adsorb CO and O_2 weakly. Also throughout our studies, we found that the reference materials Au(111)/mica and a TiO_2 film fully covering the Au(111)/mica substrate did not adsorb CO or O_2 down to 150 K. From previous UHV studies, it is known that only a fractional monolayer of CO adsorbs on Au below 125 K, oxygen is weakly chemisorbed molecularly and an activation barrier exists for dissociative O_2 adsorption.[8−11]

Also perfect TiO_2 surfaces do not adsorb significant amounts of CO.[14−17] Some adsorption can only occur in the presence of vacancy defects[18,19] and Lu et al.[53] found some desorption of CO around 150 K. Also the adsorption of oxygen is supposed not to occur on stoichiometric TiO_2 surfaces, terraces, or steps, but on surface oxygen vacancy sites[14,17,20] which is in accordance with our results.

Since neither gold nor titania alone oxidize CO significantly at low temperature, the question arises as to whether the chemisorption behavior changes if both materials are brought into intimate contact. Disagreement exists in the literature regarding CO adsorption on such gold/titania systems.[21,54] In this work, different model systems for the gold/oxide interface were presented and investigated concerning their chemisorption behavior. Powder model catalysts were used for DRIFTS, PTA, XPS, and ISS investigations and thin-film model systems for TDS, ISS, and XPS studies.

As outlined in the Results section, all flat model systems did not show any CO adsorption as revealed by XPS, ISS, and TDS. In previous studies, TDS was shown to be a very sensitive method for detecting only a fraction of a monolayer. By varying the deposition conditions, the amount of free surface gold and

the structure of the gold/TiO_2 interface could be influenced. Moreover, the surface area could be increased by using a rough film. However, in all cases no significant CO desorption was found. Considering that in AuCol1 and AuCol2 the particle diameter was around 2 and 3 nm, respectively, one should expect a decrease of the intensity of the XPS signal and especially the ion scattering signal (more surface sensitive) due to shielding of the gold atoms by adsorbed CO. Because of the small particle size of gold, a high portion of gold atoms is located at the interface and an effect in the spectra should be visible even if CO adsorption occurs on gold atoms at the interface.

However, no significant decrease of the gold signal has been observed with ISS and XPS on the thin-film model systems showing that no detectable increase of CO adsorption is found. These results are supported by recent single-crystal studies.[21,40] Using LEIS Zhang et al.[21] showed that gold on single crystalline TiO_2 adsorbs only weakly CO (upper limit of 0.05 mL of CO on Au particles for dosing at 1×10^{-6} Torr). Rainer et al.[40] reported that small gold particles on alumina under 1×10^{-5} Torr CO show only a small absorption band in infrared reflection absorption spectroscopy at 200 K compared to 100 K. Moreover, our observation that CO adsorption is not significantly influenced by the particle size and the support is in agreement with studies on other ultrathin metal film/oxide model systems. In many cases the metal shows metal sites similar to bulk surfaces.[31] Finally, it has to be stated that, although thin-film model systems were used in this work, we could prove indirectly with DRIFTS of the "high surface" area model film AuCol 2, that these model catalysts also exhibit catalytic activity in low-temperature CO oxidation.

Nevertheless, the question arises, if these observations are contradictory to the results of the powder model catalysts. For these catalysts the particle size is known to be about 2 nm. At room temperature, reversible adsorption of CO was observed by DRIFTS. The adsorption was found to be stronger on gold sites than on titania sites (Figure 9). Moreover adsorption on Ti^{4+} was only found on the in situ calcined catalyst (Figure 9), but not on the ex situ calcined catalyst which is also active for CO oxidation (Figure 8). These data are in accordance with results reported by other groups.[7,38,41] The fact that after 20 min nearly the whole amount of CO desorbed indicates that CO adsorption is very weak. This is supported by the results from pulse thermal analysis (PTA, Figures 10 and 11) revealing that CO adsorption is weak and reversible. Iizuka et al.[55] have also recently reported that CO adsorption performed in a static system with constant pressure is reversible on Au/TiO_2. XPS and ISS studies on the active Au/TiO_2 powder catalyst in UHV at 120 K showed that no significant CO adsorption occurred under vacuum conditions. All these results indicate that CO adsorption is weak and is probably not the reason for enhanced activity of supported gold catalysts in low-temperature CO oxidation.

Hence, the question arises as to whether oxygen is adsorbed on the catalysts. In the studies reported here, it was found that oxygen desorbs at higher temperatures and some Ti^{3+} forms on the surface. Pretreatment of the powder catalyst in oxygen resulted in a CO_2 peak during CO adsorption although the sample was held in an argon flow for 2 h before use in the absence of O_2. Also in the case of in situ calcination of the catalysts in oxygen, adsorbed CO_2 was detected during CO adsorption. Similarly, we found with thermal analysis that after heating the catalyst in oxygen to 743 K, CO_2 was formed in higher amounts and some species, probably carbon dioxide, remained for a limited time on the surface (Figure 11). Iizuka et al.[55] also have reported that the only part of CO which is chemisorbed irreversibly is related to CO_2 formation on the surface of gold particles. These observations indicate that oxygen is stored in the system. From single-crystal studies it is known that atomic oxygen can be produced by a variety of techniques, e.g., with ozone[8,9] or in the presence of a hot filament.[11,13] This atomic oxygen species is rather stable up to about 600 K and reacts quickly with CO. Chevrier et al.[56] showed with STM under ambient conditions that atomic oxygen restructures the gold surface. Oxygen can be adsorbed if the gold crystal is treated at high temperatures (873−973 K) in 1 bar oxygen. This process is supposed to be catalyzed by surface impurities. We assume therefore that atomic oxygen is reacting on the gold surface with CO. Indication for such a species is given by TDS (only desorption at high temperatures), DRIFTS, and the fact that more CO_2 is formed in pulse thermogravimetry after oxygen treatment. This is furthermore supported by a very recent paper by Valden et al.[58] However, it cannot be ruled out with these results that molecular oxygen is reactive as well.

Hence, the synergism between gold and titania is traced to the formation of an adsorbed oxygen species on gold under ambient conditions. Note that oxygen cannot adsorb at room temperature on gold alone due to the high activation barrier. Oxygen can adsorb on titania via vacancy sites as proposed by Frost.[57] The smaller the particle size of gold, the faster is probably the spillover of the reactive oxygen species from titania to gold because more gold atoms are located at the gold−titania interface. This is in line with the fact that smaller particles lead to a higher turnover frequency as reported by Haruta et al.[5]

It has been demonstrated in the present work that no particularly strong structural contact between the oxide and gold is necessary because dried Au/TiO_2 catalysts exhibited significant catalytic activity at low temperatures without calcination. Moreover, we have shown recently that gold particles supported on either TiO_2 or ZrO_2[25] exhibit markedly different activities. This is in accordance with our model, because different oxides are supposed to activate oxygen differently. The small gold particles are assumed to be the place where adsorbed oxygen and reversibly adsorbed carbon monoxide react, whereas the activation of oxygen occurs on the metal oxide support. Consequently we propose the following mechanism for the low-temperature oxidation of CO on Au/TiO_2:

1. Irreversible adsorption of oxygen on vacancy sites of the oxide (strongly dependent on the support):

$$\square_{\bigcirc} + O_2 + e^- \rightarrow \square_{\bigcirc}{-}O^-_{2ads}$$

$$\square_{\bigcirc} = \text{vacancy site}$$

2. Spillover of adsorbed oxygen on the gold surface (dependent on the particles size):

$$2Au + \square_{\bigcirc}{-}O^-_{2ads} \rightleftharpoons 2Au{-}O_{ads} + e^- + \square_{\bigcirc}$$

3. Reversible adsorption of CO on gold sites:

$$Au + CO \rightleftharpoons Au{-}C{\equiv}O$$

4. Reaction of CO with adsorbed oxygen (fast):

$$Au{-}C{\equiv}O + Au{-}O_{ads} \rightarrow 2Au + CO_2$$

All steps have been clarified within this work and earlier studies, except the spillover of oxygen from the metal oxide to gold. The reversible adsorption of CO on gold was extensively studied within this work. The adsorption of oxygen and its activation was proved indirectly. The fast reaction of CO with

oxygen preadsorbed gold surfaces has been reported in several studies[11,13] as well as the adsorption of oxygen on vacancy sites of TiO_2.[14,17,20] However, the nature of the oxygen species involved and the mechanism of oxygen migration from the oxide to the gold is not fully uncovered. The study of this effect is obscured by the large background of lattice O present. Electron spin resonance could identify the paramagnetic O_2^- and O^- species.

Conclusions

To gain further insight into the role of the gold/titania interface in the low-temperature oxidation of carbon monoxide, chemisorption of the reactants, CO and O_2, has been studied on structurally different Au/TiO_2 model catalysts. The combined use of powder model catalysts and thin-film model systems has been applied to overcome the "structure gap" between real catalysts and single crystals and to link results from powder catalysts with those of surface science studies. For this purpose "size-controlled" gold colloids deposited on titania powder (catalytically active, similar to powder catalysts) and titania deposited on flat Au(111)/mica films (flat, conducting model system with inversed layer structure, suitable for surface spectroscopic investigation) were applied.

Bridging the structure gap between flat model systems and powder catalysts has been furthered by a model system, which was prepared by adsorption of colloids, in analogy to the powder model catalyst. This can be regarded as alternative route to the spin coating technique proposed by other groups for such "realistic" surface science model systems, if the catalyst is composed of small metal particles on the support.

The results of the chemisorptive properties of these structurally different model systems, gained with a variety of surface analytical techniques are in line with a mechanism which assumes that oxygen is adsorbed preferentially on titania vacancy sites and reacts with CO on the small gold particles. CO adsorption was found to be weak on all model systems. Activation of oxygen is proposed to be the crucial factor in the synergism of gold and titania. Although these conclusions are supported by a very recent study by Valden et al.[58] on single-crystal surfaces, further work toward clarifying the adsorption and activation of oxygen in the $Au-TiO_2$ system at room temperature is necessary to substantiate the proposed mechanism.

Acknowledgment. Thanks are due to O. Becker (Universität Zürich) and R. Wessiken (ETH Hönggerberg) for performing the HRTEM measurements, and to P. M. Fabrizioli for helping to perform DRIFTS measurements. We also thank M. Maciejewski for thermal analysis experiments and C. Wögerbauer for measurements of the catalytic activity. Fruitful discussions, especially with U. Göbel and R. Köppel, are kindly acknowledged.

References and Notes

(1) Haruta, M.; Kobayashi, T.; Tsubota, S.; Nakahara, Y. *Chem. Express* **1988**, *5*, 349.
(2) Haruta, M.; Yamada, N.; Kobayashi, T.; Iijima, S. *J. Catal.* **1989**, *115*, 301.
(3) Knell, A.; Barnickel, P.; Baiker, A.; Wokaun, A. *J. Catal.* **1992**, *137*, 306.
(4) Lin, S. D.; Bollinger, M.; Vannice, M. A. *Catal. Lett.* **1993**, *17*, 245.
(5) Haruta, M.; Tsubota, S.; Kobayashi, T.; Kageyama, H.; Genet, M. J.; Delmon, B. *J. Catal.* **1993**, *144*, 175.
(6) Haruta, M. *Catal. Today* **1997**, *36*, 153.
(7) Bollinger, M. A.; Vannice, M. A. *Appl. Catal., B Environ.* **1996**, *8*, 417.
(8) Parker, D. H.; Koel, B. E. *J. Vac. Sci. Technol., A* **1989**, *8*, 2585.
(9) Wickham, D. T.; Parker, D. H.; Kastanas, G. N.; Lazaga, M. A.; Koel, B. E. In *Catalytic Selective Oxidation*; Oyama S. T., Hightower, J. W., Eds.; ACS Symposium Series 523; American Chemical Society, Washington, DC, 1993; p 90.
(10) Schmitz, P. J.; Kang, H. C.; Leung, W.-Y.; Thiel, P. A. *Surf. Sci.* **1991**, *248*, 287.
(11) Outka, D. A.; Madix, R. J. *Surf. Sci.* **1987**, *179*, 351.
(12) Trapnell, B. M. W. *Proc. R. Soc. London, Ser. A* **1953**, *218*, 566.
(13) Sault, A. G.; Madix, R. J.; Campbell, C. T. *Surf. Sci.* **1986**, *169*, 347.
(14) Linsebigler, A.; Lu, G.; Yates, J. T. *Chem. Rev.* **1995**, *95*, 735.
(15) Linsebigler, A.; Lu, G.; Yates, J. T. *J. Chem. Phys.* **1995**, *103*, 9438.
(16) Torquemada, M. C.; Segovia, J. L.; Roman, E. *Surf. Sci.* **1995**, *337*, 31.
(17) Göpel, W.; Rocker, G.; Feierabend, R. *Phys. Rev. B* **1983**, *28*, 3427.
(18) Kobayashi, H.; Yamaguchi, M. *Surf. Sci.* **1989**, *214*, 466.
(19) Tanaka, K.; White, J. M. *J. Phys. Chem.* **1982**, *86*, 4708.
(20) Pan, J. M.; Maschhoff, B. L.; Diebold, U.; Madey, T. E. *J. Vac. Sci. Technol., A* **1992**, *10*, 2470.
(21) Zhang, L.; Persaud, R.; Madey, T. E. *Phys. Rev. B* **1997**, *56*, 10549.
(22) Grunwaldt, J. D.; Atamny, F.; Göbel, U.; Baiker, A. *Appl. Surf. Sci.* **1996**, *99*, 353.
(23) Grunwaldt, J. D.; Göbel, U.; Baiker, A. *Fresenius J. Anal. Chem.* **1997**, *358*, 96.
(24) Duff, D. G.; Baiker, A.; Edwards, P. P. *J. Chem. Soc. Chem. Commun.* **1993**, 96.
(25) Grunwaldt, J.-D.; Kiener, C.; Woegerbauer, C.; Baiker, A. *J. Catal.*, in press.
(26) Fröhlich, C. *In-situ FTIR Studien der CO_2 Hydrierung an Kupfer/Silber-Zirkondioxid-Katalysatoren*. Dissertation, ETH Zürich, 1993.
(27) Maciejewski, M.; Müller, C. A.; Tschan, R.; Emmerich, W. D.; Baiker, A. *Thermochimica Acta* **1997**, *295*, 167.
(28) Chidsey, C. E. D.; Loiacono, D. N.; Sleator, T.; Nakahara, S. *Surf. Sci.* **1988**, *200*, 45.
(29) Rose, J. A.; Thundat, T.; Nagahara, L. A.; Lindsey, S. M. *Surf. Sci.* **1991**, *256*, 102.
(30) Izumi, K.; Murakami, M.; Deguchi, T.; Morita, A. *J. Am. Ceram. Soc.* **1989**, *72*, 1465.
(31) Campbell, C. T. *Surf. Sci. Rep.* **1997**, *27*, 1.
(32) Chatain, D.; Rivollet, I.; Eustaphopoulos, N. *J. Chim. Phys.* **1986**, *83*, 561.
(33) Ladas, S.; Poppa, H.; Boudart, M. *Surf. Sci.* **1981**, *102*, 151.
(34) Doering, D. L.; Dickkinson, J. T.; Poppa, H. *J. Catal.* **1982**, *73*, 104.
(35) Gillet, E.; Channakhone, S.; Matolin, V. *J. Catal.* **1986**, *97*, 437.
(36) Gunter, P. L. J.; Niemantsverdriet, J. W. H.; Ribeiro, F. H.; Somorjai, G. A. *Catal. Rev. Sci. Eng.* **1997**, *39*, 77.
(37) Yates, D. J. C. *J. Phys. Chem.* **1961**, *65*, 746.
(38) Boccuzzi, F.; Chiorino, A.; Tsubota, S.; Haruta, M. *Catal. Lett.* **1994**, *29*, 225.
(39) Ruggiero, C.; Hollins, P. *Surf. Sci.* **1997**, *377*, 583.
(40) Rainer, D. R.; Xu, C.; Holmblad, P. M.; Goodman, D. W. *J. Vac. Sci. Technol., A* **1997**, *15*, 1653.
(41) Boccuzzi, F.; Chiorino, A.; Tsubota, S.; Haruta, M. *J. Phys. Chem.* **1996**, *100*, 3625.
(42) Beden, B.; Bewick, A.; Kunimatsu, K.; Iamy, C. *J. Electroanal. Chem.* **1982**, *142*, 345.
(43) Tadayyoni, M. A.; Weaver, M. J. *Langmuir* **1986**, *2*, 179.
(44) Zaki, M. I.; Knözinger, H. *Spectrochim. Acta* **1987**, *43A*, 1455.
(45) Morterra, C. *J. Chem. Soc., Faraday Trans. 1* **1988**, *84*, 1617.
(46) Chang, S. C.; Hamelin, A.; Weaver, M. J. *J. Phys. Chem.* **1991**, *95*, 5560.
(47) Edens, G. J.; Hamelin, A.; Heaver, M. J. *J. Phys. Chem.* **1996**, *100*, 2322.
(48) Freund, H.-J.; Plummer, E. W. *Phys. Rev. B* **1981**, *23*, 4859.
(49) Bäumer, M.; Libuda, J.; Freund, H.-J. In *Chemisorption and Reactivity on Supported Clusters and Thin Films*; (Kluwer Academic Publishers: Dordrecht, 1997; p 61.
(50) Borg, H. J.; Oetelaar, L. C. A. v.; Niemantsverdriet, J. W. *Catal. Lett.* **1993**, *17*, 81.
(51) Jong, A. M. d.; Beer, V. H. J. d.; Veen, J. A. R. v.; Niemantsverdriet, J. W. *J. Phys. Chem.* **1996**, *100*, 17722.
(52) Thüne, P. C.; Boer, M. J. G. v. d.; Niemantsverdriet, J. W. *J. Phys. Chem.* **1997**, *101*, 8559.
(53) Lu, G.; Linsebigler, A.; Yates, J. T. *J. Chem. Phys.* **1995**, *102*, 3005.
(54) Liu, Z. M.; Vannice, M. A. *Catal. Lett.* **1997**, *43*, 51.
(55) Iizuka, Y.; Fujiki, H.; Yamauchi, N.; Chijiiwa, T.; Arai, S.; Tsubota, S.; Haruta, M. *Catal. Today* **1997**, *36*, 115.
(56) Chevrier, J.; Huang, L.; Zeppenfeld, P.; Comsa, G. *Surf. Sci.* **1996**, *355*, 1.
(57) Frost, J. C. *Nature* **1988**, *334*, 577.
(58) Valden, M.; Lai, X.; Goodman, D. W.; Science **1998**, *281*, 1647.